Traveling through the Desalting Column Spontaneously Transforms Thiolated Ag Nanoclusters from Nonluminescent to Highly Luminescent

ARTICLE *in* JOURNAL OF PHYSICAL CHEMISTRY LETTERS · JUNE 2013

Impact Factor: 7.46 · DOI: 10.1021/jz400807u

6 AUTHORS, INCLUDING:

Xun Yuan
Institute of Bioengineering and Nanotechnology
40 PUBLICATIONS **1,258** CITATIONS
SEE PROFILE

Yong Yu
Agency for Science, Technology and Research …
23 PUBLICATIONS **626** CITATIONS
SEE PROFILE

Jianping Xie
National University of Singapore
110 PUBLICATIONS **4,402** CITATIONS
SEE PROFILE

THE JOURNAL OF PHYSICAL CHEMISTRY Letters

Letter

pubs.acs.org/JPCL

Traveling through the Desalting Column Spontaneously Transforms Thiolated Ag Nanoclusters from Nonluminescent to Highly Luminescent

Xun Yuan, Qiaofeng Yao, Yong Yu, Zhentao Luo, Xinyue Dou, and Jianping Xie*

Department of Chemical and Biomolecular Engineering, National University of Singapore, 4 Engineering Drive 4, 117576, Singapore

Supporting Information

ABSTRACT: This letter reports an unexpected observation in the purification of ultrasmall (<2 nm) thiolate-protected Ag nanoclusters (NCs) via a common separation technique (e.g., desalting column and ultrafiltration), where the nonluminescent Ag NCs were spontaneously transformed to highly luminescent NCs during the separation. This interesting finding was then used to develop a facile and fast (<5 min) synthesis method for highly luminescent Ag NCs. The key strategy was to use the separation process to selectively remove small species (e.g., salts and excess protecting ligands) from the Ag NC solution, which induced a size or structure-focusing of Ag NCs in the solution, leading to the formation of highly luminescent Ag NCs. The *concurrent* synthesis and purification of highly luminescent Ag NCs via a common "physical separation unit" could be further advanced in a continuous mode for large-scale production of luminescent Ag NCs.

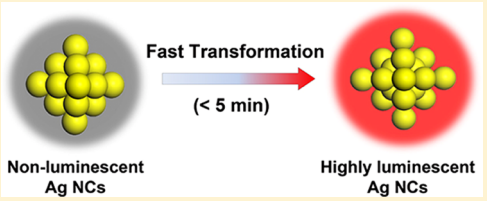

SECTION: Physical Processes in Nanomaterials and Nanostructures

In biotechnology, advanced separation techniques, such as desalting column, dialysis, and ultrafiltration, are widely used to remove low-molecular-weight substances from large biomolecules (e.g., protein and DNA).[1] Such bioseparation techniques have recently emerged as powerful methods in nanotechnology for the purification of functional nanoparticles (NPs) from small impurities (e.g., ions, excess protecting ligands, and byproducts).[2−4] The separation processes are generally considered to be inert (or have negligible effects) on the physicochemical properties (e.g., size, shape, and optical) of the as-purified NPs. This inertness feature has been well-documented in NP systems, such as metal NPs and semiconductor quantum dots (QDs).[2−5] Those NPs were typically larger than 2 nm.[6−8] However, the same (the inertness feature) may not be true if the as-separated NPs' size becomes much smaller, that is, <2 nm. Here we report an unexpected observation in the purification of ultrasmall (<2 nm) Ag NPs by using a commercial desalting column, where significant changes in the physicochemical property of small Ag NPs were observed: the nonluminescent Ag NPs were simultaneously transformed to highly luminescent counterparts when they were traveling through the column. The unique phenomenon observed in the desalting column was then used to develop a facile, fast, and large-scale synthetic method for highly luminescent Ag NPs. In addition, the highly luminescent Ag NPs synthesized by the desalting (or separation) column were readily purified from the small impurities and therefore were ready for further applications.

Our targeted materials for separation are ultrasmall Ag NPs below 2 nm in size, which are typically classified as nanoclusters (NCs).[9−11] Recently, noble-metal (e.g., Ag and Au) NCs have attracted increasing interest in the nanoscience community due to their unique size-dependent electronic and optical properties combined with their great potential in biomedical applications as bioimaging probes,[12−14] antimicrobial agents, and biosensors.[15,16] One of the most interesting features of Ag or Au NCs is their strong luminescence. Several synthetic methods for luminescent Ag or Au NCs currently exist. Examples include biomolecular (e.g., protein, peptide, and DNA)-directed method,[13,17−20] polymer [e.g., poly(methacrylic acid) (PMAA)[21,22] and poly(amidoamine) (PAMAM)]-templated method,[23,24] and thiolate ligand-mediated method.[25−30] We present a paradigm shift synthetic strategy for highly luminescent Ag NCs, where a physical separation process (e.g., desalting column or ultrafiltration) was used to facilitate a facile and fast (<5 min) synthesis of thiolate-protected Ag NCs (or thiolated Ag NCs) with strong luminescence (Scheme 1). The key strategy was to introduce a separation process to suitably remove the excess protecting ligands (thiolate ligands for example) from the Ag NC solution, stimulating a subsequent size or structure focusing,[31,32] which led to the formation of highly luminescent Ag NCs with a well-defined size and structure within *minutes*. To the best of our knowledge, this is the first demonstration of a "physical operation unit" for the fabrication of luminescent NCs. The "operation unit" can be easily modified as a *continuous* flow reactor (vs the common *batch*-mode in the current syntheses of luminescent NCs) for large-scale production of luminescent NCs in quantities large enough for application explorations.

Received: April 17, 2013
Accepted: May 13, 2013

   dx.doi.org/10.1021/jz400807u | *J. Phys. Chem. Lett.* 2013, 4, 1811−1815

Scheme 1. Schematic Illustration of the Fast Transformation (< 5 min) of the Non-Luminescent Ag NCs to Highly Luminescent Ag NCs in a Desalting Column

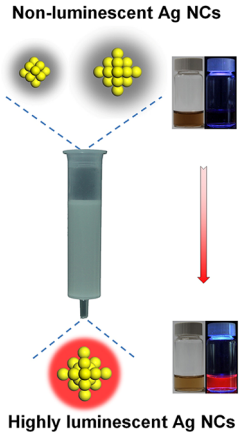

Thiolated Ag NCs were chosen as our NC model. Well-studied thiolated Ag NCs—glutathione or GSH-protected Ag NCs (GSH-Ag NCs for short) were selected in this study. GSH is a natural tripeptide containing one thiol group (from the cysteine residue). The raw GSH-Ag NCs was first prepared by a common sodium borohydride ($NaBH_4$) reduction of thiolate–Ag^I complexes, followed by an additional decomposition–reduction process.[16] The additional decomposition–reduction process was introduced to enhance the stability of the raw Ag NCs. As shown in Figure 1a (inset, no.1), the raw Ag NCs were deep-brown in solution under normal light. No luminescence was observed under UV illumination at 365 nm (Figure 1a, inset, no. 2). The raw Ag NCs showed one distinct absorption peak at 480 nm and two shoulder peaks at 332 and 640 nm (Figure 1a, black line), which are characteristic of molecular-like absorptions of ultrasmall Ag NCs.

Matrix-assisted laser desorption ionization-time-of-flight (MALDI-TOF) mass spectrometry was then used to obtain the size information of the raw Ag NCs. The resulting spectrum (Figure S1 in the Supporting Information) showed a broad peak in the range of 5310–6140 Da, implying that the raw Ag NCs had a broad size range. The broad size feature of the raw Ag NCs is due to the fast reduction of Ag ions by the strong reducing agent $NaBH_4$. The fast reduction kinetics led to the formation of mix-sized Ag NCs, similar to the observations in a previous study.[33] The representative transmission electron microscopy (TEM) image (Figure S2a in the Supporting Information) also indicated that the raw Ag NCs had sizes below 1.5 nm.

Interestingly, an obvious color change was observed when running the raw Ag NCs through a desalting column (PD-10, GE Healthcare), where the original deep-brown solution (Figure 1a, inset, no. 1) changed to reddish-brown (Figure 1a, inset, no. 3) spontaneously with their traveling inside the column. The running time inside the column was <5 min. The color change of the Ag NCs was also reflected by its optical absorption spectrum. The as-purified Ag NCs showed a distinct absorption peak at 485 nm (Figure 1a, solid red line), which was slightly red-shifted from the major absorption peak (~480 nm) of the raw Ag NCs (solid black line). In addition, the shoulder peaks at 332 and 640 nm of the raw Ag NCs (solid black line) disappeared in the absorption spectrum of the as-purified Ag NCs. The difference in the optical absorption of the raw and the as-purified Ag NCs suggested possible changes in their cluster size or structure.[19,33] More interestingly, the as-purified Ag NCs emitted an intense red luminescence under UV illumination (Figure 1a, inset, no. 4). The red-emitting Ag NCs showed an emission peak at 640 nm (Figure 1a, dotted red line), and its quantum yield was ~3.8% using Rhodamine B as the reference. The yield of red-emitting Ag NCs was determined to be ~90% (based on the amount of Ag in the precursor) by using inductively coupled plasma mass spectrometry (ICP-MS). Analysis of the luminescence decay response (Figure S3 in the Supporting Information) revealed a predominance of nanosecond components in the red-emitting

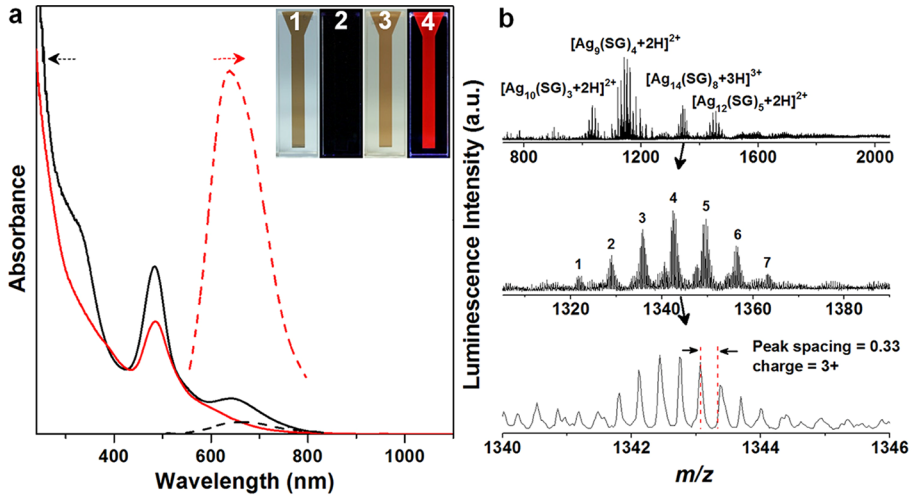

Figure 1. (a) Optical absorption (solid lines) and photoemission (dotted lines, λ_{ex} = 485 nm) spectra of the raw Ag NCs (black lines) and the resulting red-emitting Ag NCs (red lines) after running through the desalting column. Insets: photographs of the raw Ag NCs (items 1 and 2) and the red-emitting Ag NCs (items 3 and 4) taken under visible (items 1 and 3) and UV (items 2 and 4) light. (b) ESI mass spectra (in positive ion mode) of the red-emitting Ag NCs: (top) the broad-range spectrum of $Ag_M(SG)_N$, (middle) the zoomed-in spectrum of the species $[Ag_{14}(SG)_8 + 3H]^{3+}$, and (bottom) the isotope pattern of $[Ag_{14}(SG)_8 + 3Na]^{3+}$ with an observed mass of 4028.3 Da. (The calculated mass is 4029.6 Da from the molecule formula.) In the middle panel, the peak #1 corresponds to $[Ag_{14}(SG)_8 + 3H]^{3+}$, and the other peaks (#2–#7) are from the successive coordination of [+ Na–H] of peak #1.

dx.doi.org/10.1021/jz400807u | J. Phys. Chem. Lett. 2013, 4, 1811–1815

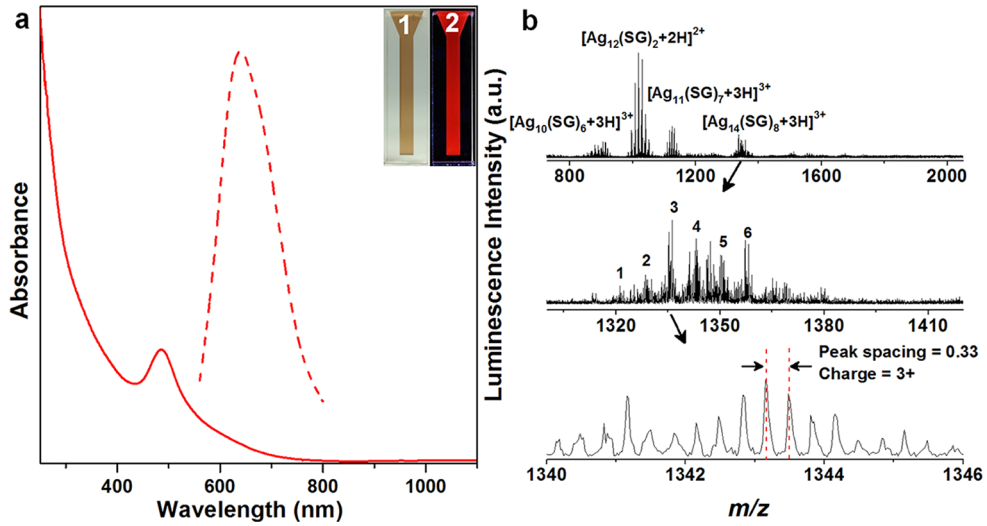

Figure 2. (a) Optical absorption (solid line) and photoemission (dotted line, λ_{ex} = 485 nm) spectra of the red-emitting Ag NCs obtained via ultrafiltration. Insets: photographs of the red-emitting Ag NCs under visible (item 1) and UV (item 2) light. (b) ESI mass spectra (in positive ion mode) of the red-emitting Ag NCs: (top) the broad-range spectrum of $Ag_M(SG)_N$, (middle) the zoomed-in spectrum of the species $[Ag_{14}(SG)_8 + 3H]^{3+}$, and (bottom) the isotope pattern of $[Ag_{14}(SG)_8 + 3Na]^{3+}$ with an observed mass of 4029.5 Da. (The calculated mass is 4029.6 Da from the molecule formula.)

Ag NCs [0.3 ns (53.5%), 1.4 ns (34.5%), and 5.2 ns (12%)]. The short lifetimes of the red-emitting Ag NCs are similar to the nanosecond emission from the singlet excited states of water-soluble Ag NCs protected by other ligands, such as polymers and DNA.[34,35] Therefore, the luminescence of the red-emitting Ag NCs was generated from the Ag core. This is distinctively different from one recent report on luminescent Au NCs,[18] which has predominant microsecond lifetime components and showed strong phosphorescence via the metal-centered triplet state. For the phosphorescent Au NCs, the thiolate-Au^I motifs on the NC surface contribute significantly to their luminescence, most likely via the aggregation-induced-emission pathway.

MALDI-TOF and electrospray ionization (ESI) mass spectrometry were used to determine the composition of the red-emitting Ag NCs. A distinct peak at ∼4000 Da was observed in the MALDI-TOF spectrum of the red-emitting Ag NCs (Figure S4 in the Supporting Information). This mass corresponds well with $Ag_{14}(SG)_8$. The ESI-MS data of the red-emitting Ag NCs further confirmed this assignment. As shown in Figure 1b (top panel), four sets of intense peaks at ∼m/z of 1032, 1141, 1342, and 1455 were observed in the m/z range of 700−2200, which were assigned to $[Ag_{10}(SG)_3 + 2H]^{2+}$, $[Ag_9(SG)_4 + 2H]^{2+}$, $[Ag_{14}(SG)_8 + 3H]^{3+}$, and $[Ag_{12}(SG)_5 + 2H]^{2+}$, respectively. The detailed assignments were presented in the middle and bottom panels of Figure 1b.[36] On the basis of the MALDI-TOF and ESI-MS analyses, the dominant species in the red-emitting Ag NCs was $Ag_{14}(SG)_8$. Other identifiable species in Figure 1b (top panel) could be the fragmentations of $Ag_{14}(SG)_8$ during the ionization, similar to the observations in previous studies.[37] Native polyacrylamide gel electrophoresis (PAGE) and thermogravimetric (TGA) analyses provided yet another line of evidence for the assignment of $Ag_{14}(SG)_8$. There was only one distinct band in the PAGE analysis of the luminescent Ag NCs (Figure S5 in the Supporting Information, inset, lane 1), and this band showed strong red emission under UV illumination (lane 2). The luminescent species isolated from the gel has similar absorption (Figure S5 in the Supporting Information, black line) and emission (red line) spectra as that of the raw luminescent product (Figure 1a, red lines), suggesting that the luminescent Ag NCs were monodisperse in size. In addition, the Ag-to-GSH ratio of luminescent Ag NCs was determined to be ∼1.74 by TGA (Figure S6 in the Supporting Information), which is consistent with the calculated value (1.75) from the cluster formula $Ag_{14}(SG)_8$. The representative TEM image (Figure S2b in the Supporting Information) also confirmed that the red-emitting Ag NCs were below 1.5 nm. A slight difference (0.07 eV) in the Ag $3d_{5/2}$ binding energy of the raw and the red-emitting Ag NCs in the X-ray photoelectron spectra (XPS) (Figure S7 in the Supporting Information) suggested the oxidation state of the Ag NCs changed after traveling through the desalting column.[38] The size and oxidation state difference of the raw and the red-emitting Ag NCs was the key to explain their remarkable optical differences (absorption and luminescence, Figure 1a). More detailed information on the luminescence origin and the cluster structure of the red-emitting Ag NCs has to await their total cluster structure determination.[39−41] It is well-accepted that some cluster features including well-defined sizes or structures are crucial for the luminescence properties of thiolated Au or Ag NCs.

The desalting columns are designed to remove small molecules like salts and ligands from large substances. In our process, the removal of small ions (e.g., OH^- and Na^+) and excess protecting ligands (GSH) suitably destabilized the Ag NCs inside the desalting column, which induced the size and structure focusing of the NCs, leading to the formation of red-emitting Ag NCs with a well-defined size and structure. No obvious changes in the optical properties (absorption and luminescence) were observed if the red-emitting Ag NCs were traveling again in the desalting column. These data suggested that a complete removal of small molecules from the Ag NC solution was achieved in the first run of separation inside the column, leading to the formation of thermodynamically stable Ag NCs. The red-emitting Ag NCs showed very good stability. As shown in Figure S8 in the Supporting Information, the luminescence loss was <10% even after 1 month of storage at 4 °C and without the protection of a N_2 blanket.

dx.doi.org/10.1021/jz400807u | J. Phys. Chem. Lett. 2013, 4, 1811−1815

Whereas it is not clear at the molecular level how the separation process in the desalting column transformed Ag NCs from nonluminescent to highly luminescent, there are two revealing experimental observations that suggested that the removal of small molecules (ions and free GSH) from the raw Ag NCs was critical for the fast formation of highly luminescent Ag NCs. First, without the separation process (by simply incubating the raw Ag NCs at room temperature), no luminescence was observed after 10 min (Figure S9 in the Supporting Information). Second, the strategy by removing small molecules to induce size and structure focusing is fairly generic, and this strategy can be extended to other separation techniques. As a proof-of-concept, we used the ultrafiltration process to treat our nonluminescent raw Ag NCs. Ultrafiltration is a separation process using membranes to purify large substances (e.g., biomolecules and NPs) by removing small impurities below the molecular weight cut off (MWCO) of the membrane. A membrane of 3000 Da MWCO was used in this study to remove small molecules (e.g., salts and free GSH) in the raw Ag NCs. Similar to our observations in the desalting column, the as-purified Ag NCs via the ultrafiltration showed strong red emission under UV illumination (Figure 2a, inset, no.2). The red-emitting Ag NCs also showed an emission peak at 640 nm (Figure 2a, dotted line), which matches nicely with the red-emitting Ag NCs synthesized by the desalting column (Figure 1a, dotted red line). The red-emitting Ag NCs synthesized by the ultrafiltration were also reddish-brown in solution (Figure 2a, inset, no.1) and showed an identical absorption spectrum (Figure 2a, solid line) as that of the red-emitting Ag NCs synthesized in the desalting column (Figure 1a, solid red line). They also have the same molecular formula of $Ag_{14}(SG)_8$ according to the MALDI-TOF (Figure S10 in the Supporting Information) and ESI-MS (Figure 2b) data. The representative TEM image (Figure S11 in the Supporting Information) also confirmed that the size of the red-emitting Ag NCs after the ultrafiltration was below 1.5 nm.

In summary, we have observed an unexpected phenomenon in the purification of thiolated Ag NCs by using a common bioseparation technique, such as desalting column and ultrafiltration cell. This interesting finding was then used to develop a simple and fast synthesis method for highly luminescent Ag NCs. The key strategy was to use the separation process to remove small molecules (salts and free protecting ligands) from the raw Ag NCs, stimulating a subsequent size or structure focusing of the NCs, which led to the formation of red-emitting Ag NCs with a well-defined size and structure. The assistance of a "physical operation unit" for the fabrication of luminescent NCs is a novel synthetic strategy, which could also be applied to other NC systems.

■ ASSOCIATED CONTENT

Supporting Information

The instrumentation used in this study and the corresponding detailed experimental procedures and supporting figures. This material is available free of charge via the Internet at http://pubs.acs.org.

■ AUTHOR INFORMATION

Corresponding Author

*E-mail: chexiej@nus.edu.sg. Tel: +65 6516 1067.

Notes

The authors declare no competing financial interest.

■ ACKNOWLEDGMENTS

This work is financially supported by the Ministry of Education, Singapore, under Grants R-279-000-327-112 and R-279-000-383-112. X.Y. acknowledges the National University of Singapore for his research scholarship.

■ REFERENCES

(1) Ward, O. *Bioprocessing*; Van Nostrand Reinhold: New York, 1991.

(2) Carney, R. P.; Kim, J. Y.; Qian, H.; Jin, R.; Mehenni, H.; Stellacci, F.; Bakr, O. M. Determination of Nanoparticle Size Distribution Together with Density or Molecular Weight by 2D Analytical Ultracentrifugation. *Nat. Commun.* **2011**, *2*, 335.

(3) Sapsford, K. E.; Tyner, K. M.; Dair, B. J.; Deschamps, J. R.; Medintz, I. L. Analyzing Nanomaterial Bioconjugates: A Review of Current and Emerging Purification and Characterization Techniques. *Anal. Chem.* **2011**, *83*, 4453−4488.

(4) Trefry, J. C.; Monahan, J. L.; Weaver, K. M.; Meyerhoefer, A. J.; Markopolous, M. M.; Arnold, Z. S.; Wooley, D. P.; Pavel, I. E. Size Selection and Concentration of Silver Nanoparticles by Tangential Flow Ultrafiltration for SERS-Based Biosensors. *J. Am. Chem. Soc.* **2010**, *132*, 10970−10972.

(5) Vaneski, A.; Susha, A. S.; Rodríguez-Fernández, J.; Berr, M.; Jäckel, F.; Feldmann, J.; Rogach, A. L. Hybrid Colloidal Heterostructures of Anisotropic Semiconductor Nanocrystals Decorated with Noble Metals: Synthesis and Function. *Adv. Funct. Mater.* **2011**, *21*, 1547−1556.

(6) Yang, J.; Ying, J. Y. A General Phase-Transfer Protocol for Metal Ions and Its Application in Nanocrystal Synthesis. *Nat. Mater.* **2009**, *8*, 683−689.

(7) Liu, H.; Qu, J.; Chen, Y.; Li, J.; Ye, F.; Lee, J. Y.; Yang, J. Hollow and Cage-Bell Structured Nanomaterials of Noble Metals. *J. Am. Chem. Soc.* **2012**, *134*, 11602−11610.

(8) Sun, Z.; Yang, Z.; Zhou, J.; Yeung, M. H.; Ni, W.; Wu, H.; Wang, J. A General Approach to the Synthesis of Gold−Metal Sulfide Core−Shell and Heterostructures. *Angew. Chem., Int. Ed.* **2009**, *48*, 2881−2885.

(9) Lu, Y.; Chen, W. Sub-Nanometre Sized Metal Clusters: From Synthetic Challenges to the Unique Property Discoveries. *Chem. Soc. Rev.* **2012**, *41*, 3594−3623.

(10) Maity, P.; Xie, S.; Yamauchi, M.; Tsukuda, T. Stabilized Gold Clusters: From Isolation toward Controlled Synthesis. *Nanoscale* **2012**, *4*, 4027−4037.

(11) Jin, R. Quantum Sized, Thiolate-Protected Gold Nanoclusters. *Nanoscale* **2010**, *2*, 343−362.

(12) Shang, L.; Dong, S.; Nienhaus, G. U. Ultra-Small Fluorescent Metal Nanoclusters: Synthesis and Biological Applications. *Nano Today* **2011**, *6*, 401−418.

(13) Choi, S.; Dickson, R. M.; Yu, J. Developing Luminescent Silver Nanodots for Biological Applications. *Chem. Soc. Rev.* **2012**, *41*, 1867−1891.

(14) Yu, M.; Zhou, C.; Liu, J.; Hankins, J. D.; Zheng, J. Luminescent Gold Nanoparticles with pH-Dependent Membrane Adsorption. *J. Am. Chem. Soc.* **2011**, *133*, 11014−11017.

(15) Yuan, X.; Luo, Z.; Yu, Y.; Yao, Q.; Xie, J. Luminescent Noble Metal Nanoclusters as an Emerging Optical Probe for Sensor Development. *Chem. Asian J.* **2013**, *8*, 858−871.

(16) Yuan, X.; Setyawati, M. I.; Tan, A. S.; Ong, C. N.; Leong, D. T.; Xie, J. Highly Luminescent Silver Nanoclusters with Tunable Emissions: Cyclic Reduction-Decomposition Synthesis and Antimicrobial Properties. *NPG Asia Mater.* **2013**, *5*, e39.

(17) Xie, J. P.; Zheng, Y. G.; Ying, J. Y. Protein-Directed Synthesis of Highly Fluorescent Gold Nanoclusters. *J. Am. Chem. Soc.* **2009**, *131*, 888−889.

(18) Luo, Z.; Yuan, X.; Yu, Y.; Zhang, Q.; Leong, D. T.; Lee, J. Y.; Xie, J. From Aggregation-Induced Emission of Au(I)−Thiolate Complexes to Ultrabright Au(0)@Au(I)−Thiolate Core−Shell Nanoclusters. *J. Am. Chem. Soc.* **2012**, *134*, 16662−16670.

(19) Negishi, Y.; Nobusada, K.; Tsukuda, T. Glutathione-Protected Gold Clusters Revisited: Bridging the Gap between Gold(I)−Thiolate Complexes and Thiolate-Protected Gold Nanocrystals. *J. Am. Chem. Soc.* **2005**, *127*, 5261−5270.
(20) Chakraborty, I.; Thumu, U. B. R.; Pradeep, T. High Temperature Nucleation and Growth of Glutathione Protected ~Ag_{75} Clusters. *Chem. Commun.* **2012**, *48*, 6788−6790.
(21) Tsunoyama, H.; Tsukuda, T. Magic Numbers of Gold Clusters Stabilized by PVP. *J. Am. Chem. Soc.* **2009**, *131*, 18216−18217.
(22) Xu, H. X.; Suslick, K. S. Sonochemical Synthesis of Highly Fluorescent Ag Nanoclusters. *ACS Nano* **2010**, *4*, 3209−3214.
(23) Zheng, J.; Petty, J. T.; Dickson, R. M. High Quantum Yield Blue Emission From Water-Soluble Au-8 Nanodots. *J. Am. Chem. Soc.* **2003**, *125*, 7780−7781.
(24) Zheng, J.; Dickson, R. M. Individual Water-Soluble Dendrimer-Encapsulated Silver Nanodot Fluorescence. *J. Am. Chem. Soc.* **2002**, *124*, 13982−13983.
(25) Udaya Bhaskara Rao, T.; Pradeep, T. Luminescent Ag_7 and Ag_8 Clusters by Interfacial Synthesis. *Angew. Chem., Int. Ed.* **2010**, *49*, 3925−3929.
(26) Bakr, O. M.; Amendola, V.; Aikens, C. M.; Wenseleers, W.; Li, Rui; Negro, L. D.; Schatz, G. C.; Stellacci, F. Silver Nanoparticles with Broad Multiband Linear Optical Absorption. *Angew. Chem., Int. Ed.* **2009**, *121*, 6035−6040.
(27) Harkness, K. M.; Tang, Y.; Dass, A.; Pan, J.; Kothalawala, N.; Reddy, V. J.; Cliffel, D. E.; Demeler, B.; Stellacci, F.; Bakr, O. M.; et al. $Ag_{44}(SR)_{30}^{4-}$: A Silver-Thiolate Superatom Complex. *Nanoscale* **2012**, *4*, 4269−4274.
(28) Negishi, Y.; Sakamoto, C.; Ohyama, T.; Tsukuda, T. Synthesis and the Origin of the Stability of Thiolate-Protected Au_{130} and Au_{187} Clusters. *J. Phys. Chem. Lett.* **2012**, 1624−1628.
(29) Kurashige, W.; Yamaguchi, M.; Nobusada, K.; Negishi, Y. Ligand-Induced Stability of Gold Nanoclusters: Thiolate *versus* Selenolate. *J. Phys. Chem. Lett.* **2012**, 2649−2652.
(30) Zhou, C.; Sun, C.; Yu, M.; Qin, Y.; Wang, J.; Kim, M.; Zheng, J. Luminescent Gold Nanoparticles with Mixed Valence States Generated from Dissociation of Polymeric Au(I) Thiolates. *J. Phys. Chem. C* **2010**, *114*, 7727−7732.
(31) Jin, R.; Qian, H.; Wu, Z.; Zhu, Y.; Zhu, M.; Mohanty, A.; Garg, N. Size Focusing: A Methodology for Synthesizing Atomically Precise Gold Nanoclusters. *J. Phys. Chem. Lett.* **2010**, *1*, 2903−2910.
(32) Qian, H.; Zhu, Y.; Jin, R. Size-Focusing Synthesis, Optical and Electrochemical Properties of Monodisperse $Au_{38}(SC_2H_4Ph)_{24}$ Nanoclusters. *ACS Nano* **2009**, *3*, 3795−3803.
(33) Kumar, S.; Bolan, M. D.; Bigioni, T. P. Glutathione-Stabilized Magic-Number Silver Cluster Compounds. *J. Am. Chem. Soc.* **2010**, *132*, 13141−13143.
(34) Díez, I.; Pusa, M.; Kulmala, S.; Jiang, H.; Walther, A.; Goldmann, A. S.; Müller, A. H. E.; Ikkala, O.; Ras, R. H. A. Color Tunability and Electrochemiluminescence of Silver Nanoclusters. *Angew. Chem., Int. Ed.* **2009**, *48*, 2122−2125.
(35) Richards, C. I.; Choi, S.; Hsiang, J.-C.; Antoku, Y.; Vosch, T.; Bongiorno, A.; Tzeng, Y.-L.; Dickson, R. M. Oligonucleotide-Stabilized Ag Nanocluster Fluorophores. *J. Am. Chem. Soc.* **2008**, *130*, 5038−5039.
(36) Gies, A. P.; Hercules, D. M.; Gerdon, A. E.; Cliffel, D. E. Electrospray Mass Spectrometry Study of Tiopronin Monolayer-Protected Gold Nanoclusters. *J. Am. Chem. Soc.* **2007**, *129*, 1095−1104.
(37) Zhu, M.; Qian, H.; Jin, R. Thiolate-Protected Au_{20} Clusters with a Large Energy Gap of 2.1 eV. *J. Am. Chem. Soc.* **2009**, *131*, 7220−7221.
(38) Yuan, X.; Tay, Y.; Dou, X.; Luo, Z.; Leong, D. T.; Xie, J. Glutathione-Protected Silver Nanoclusters as Cysteine-Selective Fluorometric and Colorimetric Probe. *Anal. Chem.* **2012**, *85*, 1913−1919.
(39) Padmos, J. D.; Zhang, P. Surface Structure of Organosulfur Stabilized Silver Nanoparticles Studied with X-ray Absorption Spectroscopy. *J. Phys. Chem. C* **2012**, *116*, 23094−23101.
(40) Jiang, D.-e. Staple Fitness: A Concept to Understand and Predict the Structures of Thiolated Gold Nanoclusters. *Chem.—Eur. J.* **2011**, *17*, 12289−12293.
(41) Duchesne, P. N.; Zhang, P. Local Structure of Fluorescent Platinum Nanoclusters. *Nanoscale* **2012**, *4*, 4199−4205.